

Speedy Two-Step Thermal Evaporation Process for Gold Electrode in a Perovskite Solar Cell

Kwangbae Kim, Taeyul Park and Ohsung Song[†]

Department of Materials Science and Engineering, University of Seoul, 163 Seoulsiripdae-ro, Dongdaemum-gu, Seoul 02504, Korea

(Received February 9, 2018 : Revised March 29, 2018 : Accepted March 29, 2018)

Abstract We propose a speedy two-step deposit process to form an Au electrode on hole transport layer (HTL) without any damage using a general thermal evaporator in a perovskite solar cell (PSC). An Au electrode with a thickness of 70 nm was prepared with one-step and two-step processes using a general thermal evaporator with a 30 cm source-substrate distance and 6.0×10^{-6} torr vacuum. The one-step process deposits the Au film with the desirable thickness through a source power of 60 and 100 W at a time. The two-step process deposits a 7 nm-thick buffer layer with source power of 60, 70, and 80 W, and then deposits the remaining film thickness at higher source power of 80, 90, and 100 W. The photovoltaic properties and microstructure of these PSC devices with a glass/FTO/TiO₂/perovskite/HTL/Au electrode were measured by a solar simulator and field emission scanning electron microscope. The one-step process showed a low depo-temperature of 88.5 °C with a long deposition time of 90 minutes at 60 W. It showed a high depo-temperature of 135.4 °C with a short deposition time of 8 minutes at 100 W. All the samples showed an ECE lower than 2.8 % due to damage on the HTL. The two-step process offered an ECE higher than 6.25 % without HTL damage through a deposition temperature lower than 88 °C and a short deposition time within 20 minutes in general. Therefore, the proposed two-step process is favorable to produce an Au electrode layer for the PSC device with a general thermal evaporator.

Key words buffer layer, speedy evaporation, evaporation rate, perovskite solar cell.

1. Introduction

Perovskite solar cell (PSC) can be classified into regular structure and inverted structure. Regular PSC structure is composed of glass/transparent conductive oxide (TCO)/electron transport layer (ETL)/perovskite/hole transport layer (HTL)/metal electrode in which electron can move to the outer circuit through TCO. The inverted PSC structure is composed of glass/TCO/HTL/perovskite/ETL/metal electrode.^{1,2)} Lots of research on the regular perovskite structure is in progress due to high energy conversion efficiency (ECE) and easy-fabrication.

Particularly, method of electrode forming is important to minimize the damage on HTL/electrode interface because electrode is deposited directly on organic HTL in the regular-type PSC manufacturing process.

Y. C. Kim et al.³⁾ have reported decrease in ECE due to damage on HTL caused by thermal energy when spiro-

OMeTAD as organic HTL is exposed in N₂ atmosphere annealing at 90 °C for 30 minutes. This gives an evidence that depo-temperature can affect ECE of PSC device during electrode deposition, and amount of damage on HTL with depo-temperature change are required to be observed according to electrode deposition condition. An expensive sputtering system including water cooling, substrate rotating, and high vacuum pumps to minimize damage on HTL had been employed, but it showed relatively low ECE.⁴⁾

As electrode forming using physical vapor deposition process lacks economic feasibility, research on carbon electrode is progressed largely to overcome the damage issue on the under layer.⁵⁻⁶⁾ Y. Shao et al.⁷⁾ reported 12.7 % of ECE when PSC was manufactured through electrode forming process without vacuum using copper tape mixed with conductive binder. F. Zhang et al.⁸⁾ reported 8.31 % of ECE using carbon electrode which can manufacture

[†]Corresponding author

E-Mail : songos@uos.ac.kr (Ohsung Song)

© Materials Research Society of Korea, All rights reserved.

This is an Open-Access article distributed under the terms of the Creative Commons Attribution Non-Commercial License (<http://creativecommons.org/licenses/by-nc/3.0>) which permits unrestricted non-commercial use, distribution, and reproduction in any medium, provided the original work is properly cited.

electrode without vacuum process. There is an advantage that the carbon-based electrode is manufactured at room temperature excluding vacuum process. However, higher ECEs have not been reported yet due to higher contact resistance than PVD processed Au electrode. For this reason, Au electrode is usually formed by using expensive customized thermal evaporator in most PSC researches.

The customized thermal evaporator used for PSC manufacturing decreases deposition rate and increased the distance between source-substrate over 60 cm to minimize damage on HTL. Expensive pump system is needed to maintain ultra-high vacuum under 1.0×10^{-6} torr to secure mean free path of gold particle during the deposition process. However, such thermal deposition method takes relatively long depo-time of about 30 min to form 70nm-thick Au electrodes due to its relatively low deposition rate. More research is needed to check possibility of Au electrode deposition without any damage on HTL/electrode interface by using existing ordinary thermal evaporator having economic vacuum pumps < 30 cm distance of source-substrate and short depo-time of < 20 minutes. Therefore, we tried to find appropriate thermal evaporation process, so called 'two-step', to lessen the depo-time and the damage on HTL by employing 7nm-thick buffer layer with an ordinary thermal evaporator consisting of 30 cm source-substrate distance.

2. Experimental Procedure

Mesoporous TiO_2 (Dyrsol DSL, 18NR-T), perovskite (sigma aldrich, PbI_2 and MAI), and spiro-OMeTAD (sigma aldrich) layers were formed on $2.5 \text{ cm} \times 2.5 \text{ cm}$ glass/FTO substrate.⁹⁾ Finally, glass/500nm-FTO/200nm- TiO_2 /500nm-perovskite/160nm-spiro-OMeTAD/70nm-Au PSC structure was manufactured by depositing 70nm-thick Au on the prepared structure as shown in Fig. 1.

Au electrode was deposited on 9 PSC samples with stainless masks attached at stainless holder of 15 cm in diameter at the same time by using a one-step process or a two-step process. The one-step process deposits the Au film through a given source power. Deposition rate was measured according to each evaporation condition. The two-step process consisted of manufacturing buffer layer with low source power and forming the remaining electrode at high energy. First, 7 nm buffer layer was formed with 60~80 W which was a relatively small amount of energy and Au electrode was deposited to become 70 nm in total by using high source power between 80 W and 100 W.

Schematic illustration of thermal evaporator used for Au electrode deposition is shown in Fig. 2. Thermal evaporator used for electrode deposition is designed to have 30 cm of distance between the Au source and the

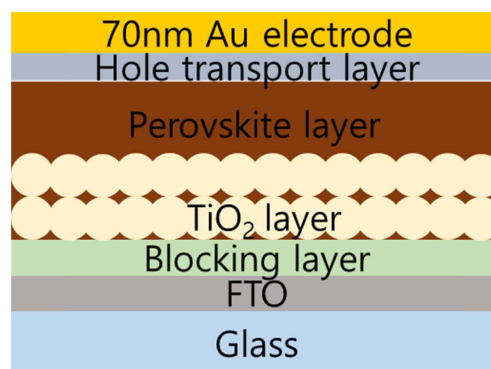


Fig. 1. Illustration of the cross-sectional structure of a perovskite solar cell.

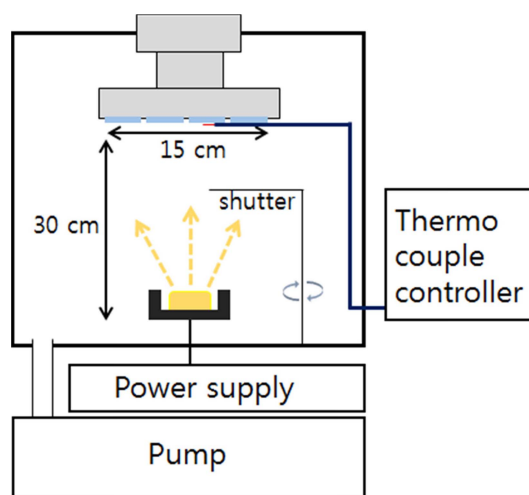


Fig. 2. Schematic illustration of a thermal evaporator employed for Au electrode deposition.

sample substrate. Pump system is composed of a rotary pump and a diffusion pump. 6.0×10^{-6} torr of vacuum was achieved by using these pumps. Au electrode deposition was started by opening shutter after stabilizing it by closing the shutter for a minute.

Thermo-couple point on glass/FTO substrate surface having the same size of with PSC tied up with polyimide tape at the center of substrate holder. Change in depo-temperature of PSC was measured every 10 seconds by using digital controller(Testo, 175T3) according to depo-time. Current-Voltage(I-V) was measured by using solar simulator(PEC-L11, Peccell) and potentiostat(Iviumstat, Ivium) to check photovoltaic properties of the final PSC. Short circuit current density(J_{sc}), open circuit voltage (V_{oc}), fill factor(FF), and ECE were also measured as well. Microstructure was analyzed with a field emission scanning electron microscope(FE-SEM, Hitachi, S-4300) to check any damage on perovskite/HTL under electrode layer after the Au electrode was selectively removed by a

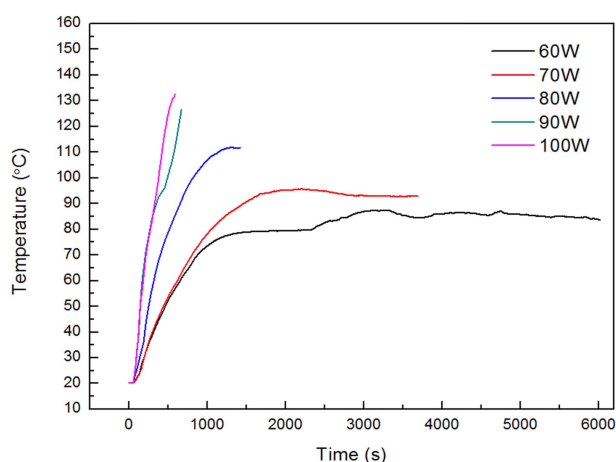


Fig. 3. Deposition temperature with deposition time and power in one step process.

tape physically.

3. Results and Discussion

Fig. 3 shows measurement result of 70 nm Au depo-time and depo-temperature according to one-step process condition with source power of 60, 70, 80, 90, and 100 W. In case of Au deposition with 60 W, 70 W of lower-power, under 100 °C of depo-temperature was measured and 90 min, 60 min of long depo-time were required while only 25 min of depo-time was required for 80 W of deposition. Meanwhile, with deposition at high-power of 90 W and 100 W, the process was finished within short depo-time (10 min and 8 min, respectively). However, there is a possibility of damage on bottom HTL when depo-temperature is over 120 °C. Therefore, low depo-temperature and long depo-time were observed when deposition was proceeded at lower power than 80 W of standard source power, while high depo-temperature and short depo-time were demanded in higher power condition.

Table 1 shows J_{sc} , V_{oc} , FF, and ECE as source power,

depo-time, maximum temperature, and photovoltaic properties when one-step process or two-step process was employed. In case of 70 nm Au deposition through 60 W one-step process, 90 min of depo-time was required. Low ECE of 1.70 % was achieved by 100 min of depo-time at 88 °C of depo-temperature as shown in Fig. 3.

With the two-step process of 60W-80W and 60W-90W, the manufactured PSC had 7 nm of buffer layer deposition for 5 min. For the remaining layer, the deposition time was 23 min and 9 min at maximum temperature of 79 °C and 74.2 °C, respectively. These temperatures were lower than the depo-temperature from the one-step process at 60 W. Improved ECE was observed as this improvement of the depo-temperature led to increase J_{sc} and FF.

In the two-step process with 70W-80W and 70W-90W, PSC was manufactured by depositing 7 nm of buffer layer within 4 min. The remaining electrode thickness was deposited for 20 min and 6 min at maximum temperature of 75.6 °C and 66.2 °C, respectively. Depo-temperature was found to be lower than the temperature from the one-step process at 70 W. ECE values of 8.33 % and 7.89 % were observed through improvement in depo-time and depo-temperature by using the two-step process.

In the two-step process with 80W-90W and 80W-100W, PSC was manufactured by depositing 7 nm of buffer layer within 3 min. The remaining electrode thickness was deposited for 11 min and 5 min, respectively. Maximum temperatures of the manufactured PSC were shown to be 87.4 °C and 57.7 °C, which is lower temperature than 115 °C from the one-step process at 80 W. ECE values of 6.47 % and 7.52 % were observed through improvement in depo-time and depo-temperature by using the two-step process. Meanwhile, with the one-step process at 100 W, low ECE of 2.87 % was observed despite its short depo-time due to increase of temperature to 135.4 °C caused by high source power.

Fig. 4 shows a graph of expected and experimentally measured temperature change of the two-step process. The expected temperature was based on the temperature

Table 1. Photovoltaic properties of PSCs with various one-step and two-step processes.

Power (W-W)	Depo-time (min)	max temp (°C)	J_{sc} (mA/cm ²)	V_{oc} (V)	FF	η (%)
60	90	88.5	6.96	0.81	0.30	1.70
60-80	28(5-23)	79.0	12.54	1.01	0.49	6.25
60-90	14(5-9)	74.2	17.11	1.02	0.55	9.56
70-80	24(4-20)	75.6	17.01	1.00	0.49	8.33
70-90	10(4-6)	66.2	14.77	1.02	0.52	7.89
80-90	14(3-11)	87.4	14.90	1.01	0.43	6.47
80-100	8(3-5)	57.7	16.85	0.99	0.45	7.52
100	8	135.4	11.20	0.75	0.34	2.87

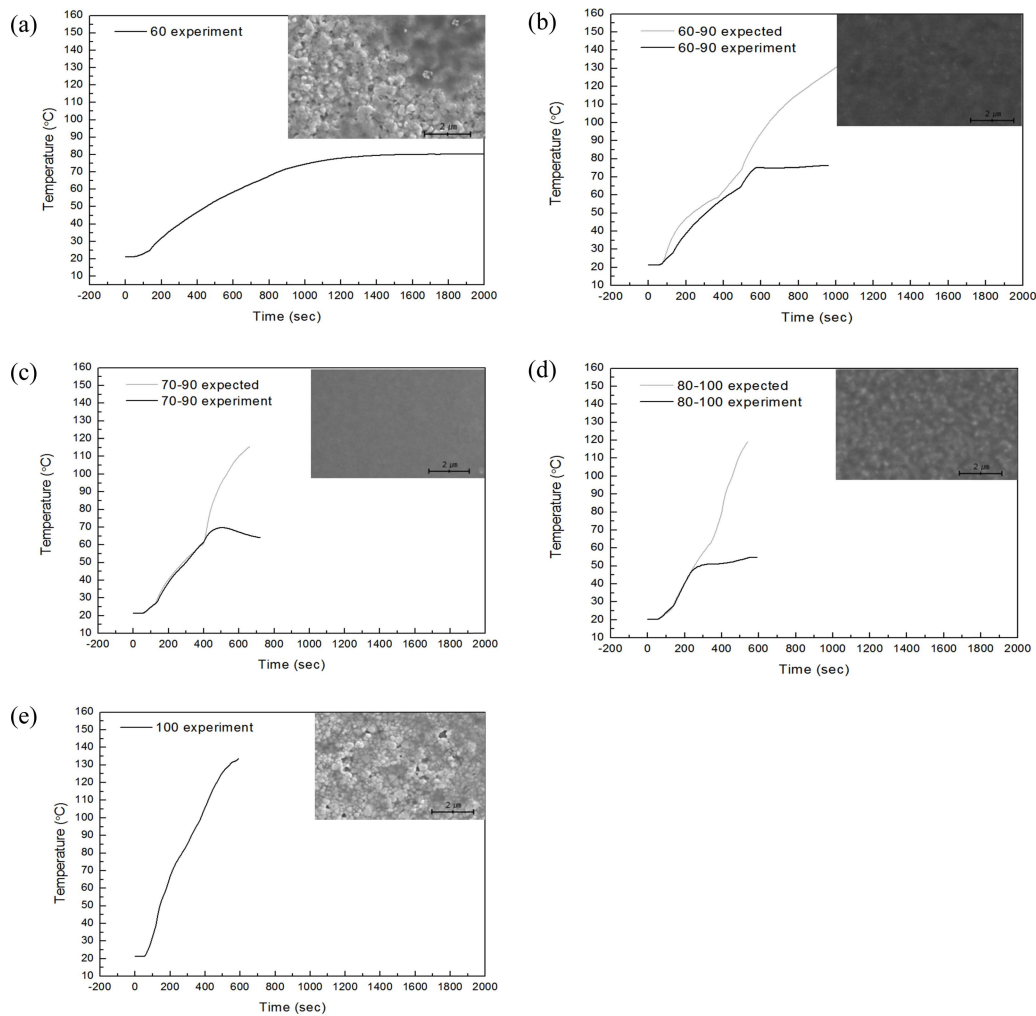


Fig. 4. Surface Temperature according to different evaporation conditions of (a) 60 W, (b) 60W-90W, (c) 70W-90W, (d) 80W-100W, and (e) 100 W. Insets are FE-SEM images of given condition.

change of one-step process at given conditions shown in Fig. 3. On the right top, microstructure of the HTL/perovskite layer after Au electrode was removed at a given process condition was shown.

Fig. 4(a) shows the result of 60 W one-step process by depo-temperature up to 2000sec when 70 nm Au was deposited on PSC. Final depo-time was required as about 100 min as shown in Fig. 3. The SEM image on the right top shows that the bottom HTL and perovskite layer were damaged by long depo-time. This problem corresponded to PSC degradation by thermal damage from the deposition process as reported by K. Kim, et al.¹⁰⁾

Fig. 4(b) shows result of the two-step process at 60W-90W. Increase in depo-temperature was expected according to change in source power to high power from low power in a grey line plot as expected temperature change of 60W-90W. However, the rate of increase in depo-temperature was decreased as in a black line plot indi-

cating actual measurement of 60W-90W. This phenomenon was judged that deposition of 7 nm buffer layer with low energy made a difference in depo-temperature change. In case of two-step process, shortening total depo-time and decrease in depo-temperature were observed eventually. On the right top, the result of SEM microstructure image shows no damage on HTL of the bottom of the electrode layer.

Fig. 4(c) shows the result of change in temperature from 70W-90W two-step process. Increase in depo-temperature was expected as well according to increase in source power to high power from low power in a grey line plot as expected temperature change of 70W-90W. However, the rate of increase in depo-temperature was decreased according to change in source power in a black line plot. Moreover, the microstructure image shown on the right top confirmed no damage on HTL of the bottom of the electrode layer.

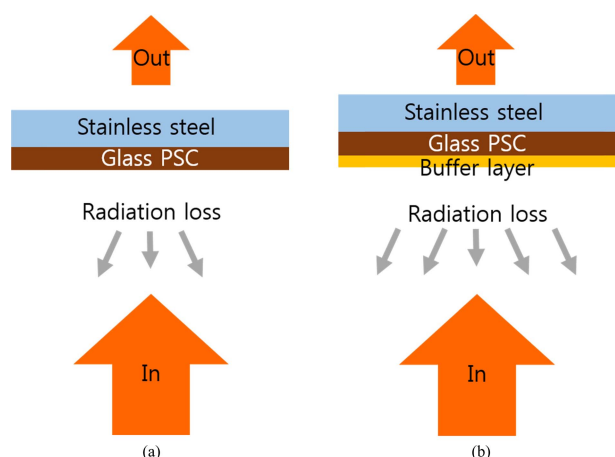


Fig. 5. Schematic illustration of the heat balance of PSC (a) without buffer layer and (b) with 7nm-thick Au buffer layer.

Fig. 4(d) shows the result of change in temperature from the 80W-100W two-step process. Increase in depo-temperature was expected according to increase in source power in the grey line plot. However, the rate of increase in depo-temperature was decreased drastically in the black line plot. Microstructure analysis result shown on the right top confirmed no damage on HTL of the bottom of the electrode layer.

Fig. 4(e) shows the result of the 100 W one-step process. Depo-temperature increased up to 135.4 °C, and decrease in ECE due to HTL and perovskite layer damage as shown in SEM microstructure inset on the right top. Therefore, decrease in maximum temperature and shortening of depo-time were possible with the proposed two-step process. Higher ECE was achieved when two-step process was employed compared to that with the one-step process.

In Fig. 5, schematic illustration was shown for explanation of mechanism about more decreasing depo-temperature in two-step process containing 7 nm buffer layer than one-step process. Transfer of general thermal energy is possible through three methods of conduction, convection, and radiation.

We assumed that heat input during thermal evaporation and heat conduction through the stainless steel holder contacting the PSC is the same. Convection is negligible as the evaporator is in a vacuum.

Radiation is proportionally emitted to $\epsilon\Delta T^4$ at the substrate surface, where ΔT is $T_{\text{substrate}} - T_{\text{environment}}$.¹¹⁾ Here ϵ represents emissivity of the PSC surface.

Fig. 5(a) shows accumulated thermal energy until Au layer becomes 70 nm in one-step process while each of Au particle has certain thermal energy evaporated from the source. At this point, thermal losses occur by conduction and radiation, and depo-temperature will indicate

the difference in thermal energy and thermal losses at the PSC surface.

Fig. 5(b) is the case of two-step process containing 7 nm buffer layer. Thermal input energy is assumed to be the same since PSC device has identical structure in Fig. 5(a). Similar amount of heat conduction loss through stainless steel holder occurred with Fig. 5(a) regardless of the 7nm-thick Au buffer layer.

On the other hand, radiation thermal loss was relatively large proportional to ΔT^4 since ΔT at the pre-produced buffer layer is greater than the temperature difference in Fig. 5(a). For this reason, the result confirmed that depo-temperature can be maintained relatively lower eventually due to the larger amount of thermal radiation losses by buffer layer than the thermal energy shown in Fig. 5(a).

Therefore, two-step process using 7 nm buffer layer could increase ECE effectively by protecting HTL of PSC as it suggested before.

4. Conclusions

We prospered two-step process that is creating 7nm-thick buffer layer with relatively low power and is depositing 70 nm thickness Au electrode in total with high power in short period of time through the ordinary thermal evaporator. Two-step process overcame the one-step process problems on long depo-time, high depo-temperature, and degradation of HTL and perovskite layers. We confirmed two-step process could proceed deposition without any under layer damage on 70 nm Au electrode within 10 min over maintaining 88 °C of depo-temperature. The two-step process using an ordinary thermal evaporator was favorable in making an Au electrode for PSC compared to the one-step process.

Acknowledgement

This research was supported by Basic Science Research Program through the National Research Foundation of Korea(NRF) funded by the Ministry of Education(2017-R1D1A1B03029347).

References

1. Y. Zhao, A. M. Nardes, and K. Zhu, *Faraday Discuss.*, **176**, 301 (2014).
2. T. Liu, K. Chen, Q. Hu, R. Zhu, and Q. Gong, *Adv. energy mater.*, **6**, 1600457 (2016).
3. Y. C. Kim, T. Y. Yang, N. J. Jeon, J. Im, S. Jang, T. J. Shin, H. W. Shin, S. Kim, E. Lee, S. Kim, J. H. Noh, S. I. Seok, and J. Seo, *Energy Environ. Sci.*, **10**, 2109 (2017).
4. L. Wang, G. R. Li, Q. Zhao, and X. P. Gao, *Energy*

- Storage Mater., **7**, 40 (2017).
5. Z. Liu, T. Shi, Z. Tang, B. Sun, and G. Liao, *Nanoscale*, **8**, 7017 (2016).
 6. M. Duan, Y. Rong, A. Mei, Y. Hu, Y. Sheng, and Y. Guan, *Carbon*, **120**, 71 (2017).
 7. Y. shao, Q. Wang, Q. Dong, Y. Yuan, J. Huang, *Nano energy*, **16**, 4 (2016).
 8. F. Zhang, X. Yang, H. Wang, M. Cheng, J. Zhao, and L. Sun, *ACS Appl. Mater. Interfaces*, **6**, 16140 (2014).
 9. N. Y. Ahn, D. Y. Son, I. H. Jang, S. M. Kang, M. S. Choi and N. G. Park, *J. Am. Chem. Soc.*, **137**, 8696 (2015).
 10. K. Kim, T. Park, and O. Song, *Korean J. Met. Mater.*, **56**, 321 (2018).
 11. Yunus A. Cengel, *Heat transfer*, 2nd ed., p.28, McGraw-Hill, USA (2002).